MICROSTRUCTURE AND DUCTILE FRACTURE OF A QUENCHED AND TEMPERED STEEL

R. Ebner, K.L. Maurer
Institut für Metallkunde und Werkstoffprüfung,
Montanuniversität Leoben

Experiments indicate that the achievement of a maximum in toughness (J_{IO}) and ductility (true strain at fracture) coincide with a spheroidization of the carbides. Further tempering decreases the strength whereas toughness and ductility vary only slightly.

The influence of inclusions was studied at specimens with different inclusion contents and distributions. During straining inclusions act as microscopic stress and strain raisers which cause an exceeding of the martensite's strain to fracture at low macroscopic strains.

INTRODUCTION

It is well known that the properties of a material are related to its microstructure. Whereas the role of structure on the strength is well understood, there are large problems in understanding toughness and ductility in terms of the structure. One reason may be that there exist a lot of different toughness criterions - e.g. ductility in the tensile test, fracture toughness, impact work etc.

In all of these parameters the deformability of the material to fracture is involved. Microscopic fracture, in the ductile regime, is always the same process that can be divided into three parts, these are 1) nucleation of voids
2) growth of voids until the
3) coalescence of voids
leads to final fracture (1,2,3,4). The nucleation of voids usually occurs at second phase particles (1-8). Because of the different deformation behaviour of particles and metallic matrix these particles are preferred sites of local stress and strain concentrations which result finally in a decohesion of the particle/matrix interface (3,6-10) or in fracture of the particles (3,7, 9-11).

In a quenched and tempered steel there act two types of particles, namely large particles (nonmetallic inclusions) and small particles (carbide precipitates). They lead to the following fracture process.

Firstly, nucleation of voids at large inclusions even at low strains (ε nucleation <0,1...0,25 (9,12-15)) depending on strength

of the material).
Secondly, in the vicinity of these voids, they act as small notches or cracks, stress and strain concentrations occur through which thirdly the nucleation of voids at carbides begins, if their void nucleation strain is exceeded.
Fourthly, the coalescence of these voids then causes final fracture of the specimen.

In high strength steels the coalescence often occurs in small highly deformed shear bands (1,9,16,17), this phenomenon is called void sheet mechanism (9). It is obvious that linking the voids at the inclusions by this mechanism is accompanied by a reduction in macroscopic strain and therefore by a loss in ductility and toughness. This process is favoured, if the precipitated particles contribute significantly to the strength of the material. If a void is formed, this particle can no longer act as an obstacle to moving dislocations combined with an increased load at neighbouring particles.

All the mechanisms discussed above depend on the stress state of the specimen which influences not only the nucleation but also the growth of voids. An increase in hydrostatic stress always decreases the void nucleation strain (5,8,11,13). The growth of voids ist determined essentially by the deformation field (18,19, 20), but deformation itself is determined by the stress state.

All these effects in sum cause a reduction of the strain to fracture (9,12,21) by increasing hydrostatic stress, Hahn and Rosenfield (22) took one third of the strain to fracture in a tensile test in their fracture toughness model.

EXPERIMENTAL DETAILS

The materials used in this investigation were conventionally melted high strength steels with chemical compositions shown in table 1.

TABLE 1 - Chemical compositions in weight percent

	C	Si	Mn	Cr	Ni	Mo	Cu	P	S
series 1	0,32	0,29	0,45	1,47	1,45	0,07	0,23	0,024	0,014
series 2,3,4	0,32	0,32	0,43	1,43	1,46	0,16	0,18	0,020	0,024

The heat treatment consisted of austenitizing for 1 hour at 870 C followed by a rapid quench in oil. Tempering conditions were tempering at 450 C and 550 C for 1 hour and tempering at 650 C for 1 to 336 hours to produce various carbide dispersions. After tempering the specimens were rapidly cooled in water.

The influence of nonmetallic inclusions was studied at four series with different inclusion contents and distributions produced by various chemical compositions and hot rolling or forging.

Measuring of inclusion length distribution and the areal distribution of the sectioned carbides was conducted by an Omnicon

Image Analysis System. The field investigated for measuring inclusion length distribution was at least 12 mm^2. Scanning electron microscopy micrographs from polished and slightly etched (with alcoholic picric-nitric acid solution) specimen were the basis for the determination of carbide size distributions, using Saltykov's stereological method (23) for calculating the spatial carbide size distributions from the distributions of sectioned areas.

Mechanical properties, measured by using a Zwick tensile testing machine, were measured by tensile and J-integral experiments. Merkle's and Corten's (24) recommendation was used for determining J-values by means of 10 mm thick CT-specimens. The critical J_{IO}-value, at the onset of stable crack extension, was taken as the J-value at the intersection of the plastic blunting curve $J=2.\sigma_{flow}.\Delta a$ with the J_R-curve. Heat tinting marked the stable crack extension.

THE ROLE OF CARBIDES IN THE TEMPERED MARTENSITE

The structure of the tempered martensite is variing due to tempering temperature in a way shown in Fig. 1.

In our investigation tempering at medium and high temperatures was performed. Carbide precipitates are embedded in a metallic matrix consisting of martensite laths and packets. As a result of heat treatment the following microstructural variants were produced.

Tempering at 450 C: This treatment causes plate-like carbides at martensite laths and packet boundaries. The high martensite dislocation density is not reduced significantly.
Tempering at 550 C: The precipitated carbides are partly spheroidized.
Tempering at 650 C: Most of the carbides have predominantly spherical shape and a reduction in dislocation density due to recovery is observable. The carbide size was varied by using different tempering times, the carbide dispersions are shown in Fig. 2a, tempered for 1 hour and in Fig. 2b, tempered for 336 hours.

The mechanical properties of the materials are listed in table 2 and the true stress - true strain behaviour is shown in Fig. 3.

Recent investigations emphasized the role of carbides in the fracture process (3,4,7-9,25), especially their influence on void nucleation (3,4,8,9) and growth (3,4) during tensile testing. Accordingly it can be assumed that elongated particles (7,26), large particles (3,8,27,28) and closely spaced particles (8,10, 29) have a detrimental effect on the ductility and toughness, additional, electron optical investigations (10) on the same material have shown the carbides at boundaries as preferred sites of void nucleation. The dominating failing mechanism depends on shape, plate-like carbides are often breaking, whereas spheres often fail by decohesion of the particle/matrix interface.

TABLE 2: Tensile properties and carbide sizes of series 2
(for series nomenclature see table 1)

tempering temperature [C]	tempering time [h]	$R_{p0.2}$ or R_{eL} [N/mm^2]	Rm [N/mm^2]	$\varepsilon_{long.}$	$\varepsilon_{trans.}$	mean carbide diameter [µm]
450	1	1240	1380	0,73	0,16	-
550	1	1120	1220	0,86	0,23	-
650	1	930	1040	1,05	0,33	0,063
	2,5	860	990	1,06	0,40	0,070
	7	810	950	1,06	0,43	0,072
	15	770	900	1,08	0,43	0,085
	41	700	820	1,10	0,43	0,111
	120	630	750	1,11	0,43	0,118
	336	580	700	1,10	0,51	0,144

Fracture surface investigation (10) of specimens with plate-like carbides indicate intercrystalline fracture paths along lath or packet boundaries due to the carbide plates lying at these boundaries. The increase of the degree of spheroidization results in vanishing this fracture mode.

Carbide spheroidization coincides with a maximum in ductility (Fig. 4) and toughness (Fig. 5). This is effected by both beneficial carbide shape and lower strength caused by a reduction in the dislocation density. According to Argon and Im (8) the stress is at the particle/matrix interface not only a function of the specimen's stress state $\sigma_m(\varepsilon_{pl})$ but also of the local stress $\sigma_l(\varepsilon_{pl})$ due to dislocation-particle interaction.

$$\sigma_{interface} = \sigma_m(\varepsilon_{pl}) + \sigma_l(\varepsilon_{pl}) \qquad \text{eq. 1}$$

The normal stress criterion means that decohesion of the interface or cracking occurs, if the stress is exceeding a critical value, the interface or the particle strength. Void nucleation at carbides takes place at higher strains than at nonmetallic inclusions. Le Roy et al. (4) and Fisher and Gurland (6) found strains to nucleation of about ε = 0,5...0,7 in tensile specimens, whereas Inoue and Kinoshita (3) reported a dependence of the particle distance.They found nucleation strains between 0,2 and 0,8. The lower value is true for larger particle distances.

A comparison of the results of our investigation with former (4,6,25) shows an excellent agreement of the ductility, by taking the volume content of second phase particles as comparing parameter, although the strength in our investigation is up to twice the strength in the other investigations. Coarsening of carbides, due to long tempering times at 650 C, decreases the strength (larger carbide distances) as shown in Fig. 6, whereas the toughness (Fig. 5) and the ductility (Fig. 4) vary only slightly.

Therfore the following conclusion can be drawn. Maximal ductility is maintained,if most of the particles reach spheroidal shape. Coarsening reduces the strength but has no significant influence on toughness and ductility.

Another problem raises by observing the toughness. It can be assumed to simplify matters that the processes at the crack tip are similar to those in a tensile test, but they occur at lower strains; we are far away from an understanding of fracture toughness. Some models were developed in the past to find a connection between microstructure, tensile properties and the toughness of a material. The basis in understanding is the knowledge of the strain distribution ahead of the crack tip, which depends on strength of the material and stress intensity. High strength means a small plastic zone combined with small strains at the crack tip. As a critical strain value at the crack tip a fraction of the tensile strain to fracture will be introduced in the calculations. Further it was found that the strain hardening behaviour has a strong influence on toughness (22,30,31). One of the best known relationships between K_{IC} and tensile properties is the model developed by Hahn and Rosenfield (22)

$$K_{IC} = \sqrt{\frac{2}{3} \cdot E.\sigma y.n^2.\varepsilon_f.25,4 \text{ [mm]}} \qquad \text{eq. 2}$$

by which K_{IC} values can be predicted well. In equation 2 E is the elastic modulus, σy and n are the yield stress and the strain hardening exponent (Ludwik) and ε_f is the true strain to fracture in a tensile test. Fig. 7 shows a comparison of measured K_{IJ} and predicted K_{IC} values. Fig. 7 includes also K_{IJ} - values from Fig. 8 given by different inclusion orientation.

THE ROLE OF NONMETALLIC INCLUSIONS

Low tensile strength and weak interfacial bonding (14) of inclusions are the reason for void nucleation at low strains.

Those voids act like small cracks accompanied by highly localized stresses and strains depending on content, size, shape, distance and orientation to deformation axis. Whilst the material strength is not influenced by inclusions, toughness and ductility are very sensitiv parameters for impurities. Marked reductions of toughness and ductility are the result, if large inclusions are present in the material. In this investigation oriented inclusions, like manganese sulfides, cause anisotropic properties as shown in Fig. 8 and Fig. 9.

As a first hypothesis it can be assumed that fracture occurs, if the fracture strain of tempered martensite is exceeded at any point of the specimen, at the stress conditions given in this place. From the reduction in strain to fracture in transversal direction a strain intensification factor due to inclusions between 2 and 4 can be calculated (Fig. 9). A model, developed by Fujita et al. (32,33), describing the influence of small noninteracting cracks on the ductility,predicts the following relationship,

$$\varepsilon_f = \text{cst.} \frac{1}{l^{1/(1+n)}} \qquad \text{eq. 3}$$

where l is the length of the inclusion and n is the strain hardening exponent. The constant in equation 3 can be estimated for the case of small scale yielding to cst = $(K_{IC}/\pi.\sigma_y)^{1/(1+n)}$, which shows the importance of matrix toughness K_{IC}, the yield stress and the strain hardening exponent. From Fig.9 and Fig.10 can be seen that series 4, which has shorter inclusions than the series 2 and 3, has the better transverse ductility.
It can be argued that amongst the inclusion length the distance between adjacent inclusions plays a dominant role, especially because the inclusions will be concentrated in the interdendritic space during solidification.

The appreciable improvement in transverse ductility of series 1 (Fig. 9) can therefore be explained by two possible factors. Firstly by reduction in inclusion length (Fig. 10) and inclusion content (the sulfur content is lower in series 1 and therefore by an enlargement of the inclusion distances or secondly by a lower molybdenum content in series 1 which possibly increases the fracture toughness. The lowering of the molybdenum content is connected with a reduction in strength of the matrix material in our case of about 8 percent compared to the other series. But these open points should be discussed in a further paper.

Another problem rises from comparing series 2 und 4. Whereas the ductility of series 4 is better than that of series 2 (because of shorter inclusions in series 4, Fig. 10), the toughness in the directions LS and ST is even lowered slightly in series 4. This effect cannot be understood well too with the present results, and will be part of a further paper.

CONCLUSION

The correlation between microstructure and some mechanical properties was studied. From the results of this investigation it can be decided that an optimal strength to toughness (or ductility) ratio is obtained, when most of the precipitated carbides are nearly spheres in shape. Further tempering causes decreasing strength,toughness and ductility hardly change.

Elongated inclusions, manganese sulfides, cause strong anisotropic toughness and ductility, which can be partly explained by length and distance to the nearest neighbour of the inclusions. But at the same time the toughness, the strength and the strain hardening behaviour of the tempered martensite must be taken into account.

ACKNOLEDGEMENT

The Fonds zur Förderung der wissenschaftlichen Forschung in Österreich is greatfully thanked for sponsoring this investigation (Projects S 14-08, S 14-02, S 14-12)

REFERENCES

1. Bucher,J.H.,Powell,G.W.,and Spretnak,J.W.,1960,Trans.Met. Soc.AIME 218,498.

2. Gurland,J.,and Plateau,J.,1963,Trans.ASM 56,442.
3. Inoue,T.,and Kinoshita,S.,1977,Trans.ISIJ 17,523.
4. LeRoy,G.,Embury,J.D.,Edward,G.,and Ashby,M.F.,1981, Acta Met. 29,1509.
5. Broek,D.,1973,Eng.Fract.Mech.5,55.
6. Fisher,J.R.,and Gurland,J.,1981,Met.Science 15,185.
7. Curry,D.A.,and Pratt,P.L.,1979,Mat.Sci.Eng.37,223.
8. Argon,A.S.,and Im,J.,1974,Met.Trans.6A,839.
9. Cox,T.B.,and Low,J.R.,Jr.,1974,Met.Trans.5,1457.
10. Ebner,R.,Schäffer,H.,and Fischmeister,H.F.,1981,Prakt. Metallographie 18,461.
11. Gurland,J.,1972,Acta Met.20,735.
12. Lautridou,J.C.,and Pineau,A.,1981,Eng.Fract.Mech 15,55.
13. Melander,A.,and Steninger,J.,1982,Mat.Sci.Eng. 52,239.
14. Beremin,F.M.,1981,Met.Trans.12A,723.
15. Roberts,W.,Lehtinen,B.,Easterling,K.E.,1976,Acta Met. 24,745.
16. French,J.E., and Weinrich,P.F.,1979,Met.Trans.10A,297.
17. Smith,E.,Cook,T.S.,and Rau,C.A.,1977,"Fracture 1977",Volume 1, ICF4,Waterloo,Canada,215.
18. Perra,M.,and Finnie,I.,1977,"Fracture 1977",Volume 2, ICF4, Waterloo,Canada,437.
19. McClintock,F.A.,1968,Trans.ASME,Journ.Appl.Mech.,June 1968, 363.
20. Rice,J.R.,and Tracey,D.M.,1969,Journ.Mech.Phys.Solids 17,201.
21. Mackenzie,A.C.,Hancock,J.W.,and Brown,D.K.,1977,Eng.Fract. Mech.9,167.
22. Hahn,G.T.,and Rosenfield,A.R.,1968,ASTM STP 432,5.
23. Saltykov,S.A.,1974,"Stereometrische Metallographie",VEB Deutscher Verlag für Grundstoffindustrie Leipzig.
24. Merkle,J.R.,and Corten,H.T.,1974,Trans.ASME,Journ.of Pressure Vessel Techn. 96,286.
25. Fukui,S.,and Uehara,N.,1970,Proc.2nd Int.Conf.on Strength of Metals and Alloys, Asiloma USA,626.
26. Gladman,T.,Holmes,B.,and McIvor,I.D.,1971,"Effect of Second Phase Particles on the Mechanical Properties of Steel",The Iron and Steel Institute, London.
27. Low,J.R.Jr.,1974,"Prospects of Fracture Mechanics",edited by Sih,Elst,Broek,51.
28. Kunio,T.,Shimizu,M.,and Kobayashi,Y.,1977, "Fracture 1977", Volume 2, ICF4,Waterloo,Canada,395.
29. Goldenberg,T.,Lee,T.,D.,and Hirth J.P.,1978,Met.Trans.9A,1663.
30. Steigerwald,E.A.,and Hanna,G.L.,1968,Trans.AIME 242,320.

31. Knott,J.F.,1975,"Mechanics and Physics of Fracture",Inst.of Physics and Metals Society,Cambridge,86.

32. Fujita,T.,Mizuta,A.,and Tsuda,O.,1977,"Fracture 1977",Volume 3, ICF4,Waterloo,Canada,437.

33. Fujita,T.,Mizuta,A.,and Tsuda,O.,1980,Int. Journ.of Fracture 16, 221.

34. Baker,T.J.,and Charles,J.A., 1971,"Effect of Second Phase Particles on the Mechanical Properties of Steel", The Iron and Steel Institute,London.

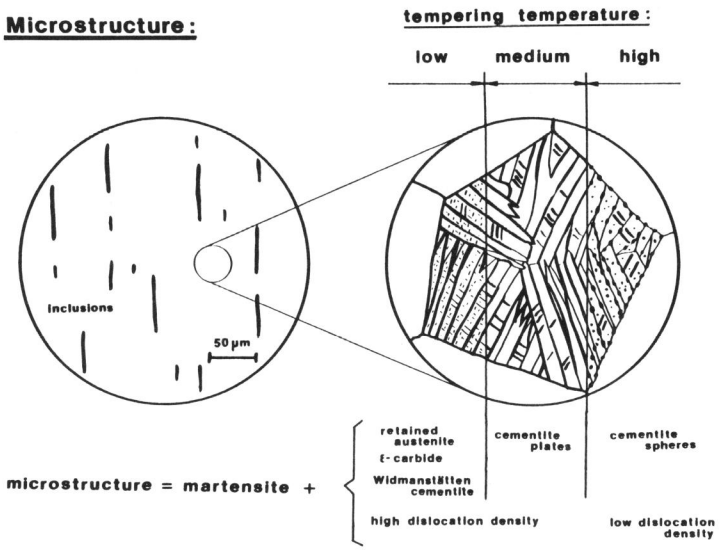

Fig.1: Possible types of microstructures depending on tempering temperature

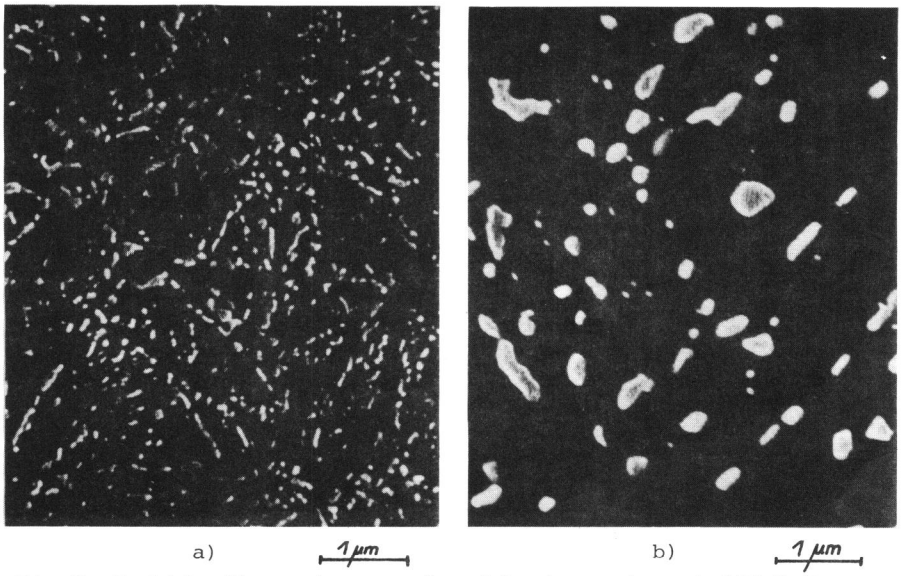

Fig.2: Carbide dispersions produced by tempering at 650 C for a) 1 hour and b) 336 hours

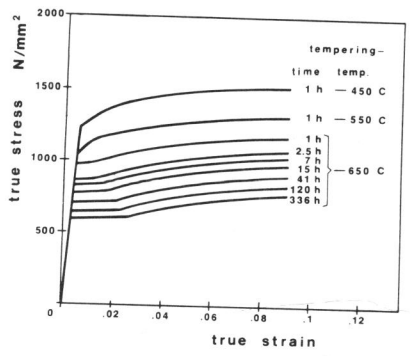

Fig.3: True stress-true strain curves for various tempering conditions

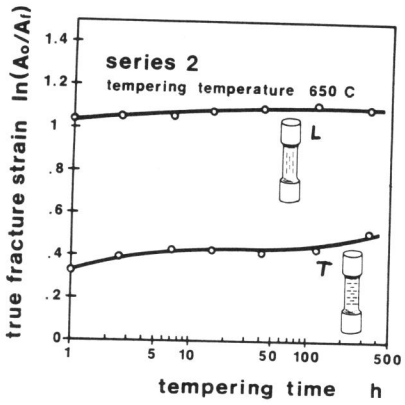

Fig.4: Ductility of different orientated specimens, temp.temperature 650C

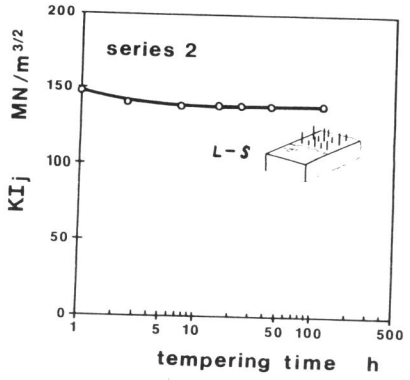

Fig.5: Toughness in LT direction, tempering temperature 650 C

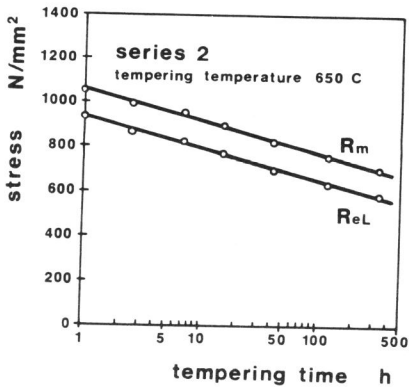

Fig.6: Tensile strength and lower yield stress, tempering temperature 650C

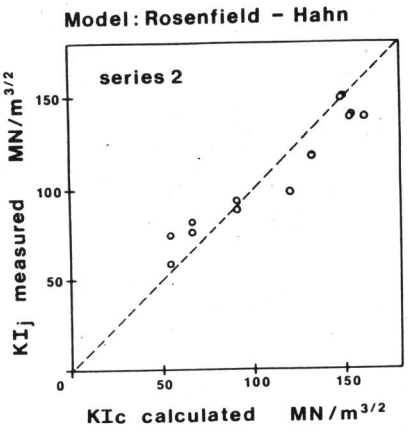

Fig. 7: Comparison of measured K_{IJ} with calculated K_{IC} values

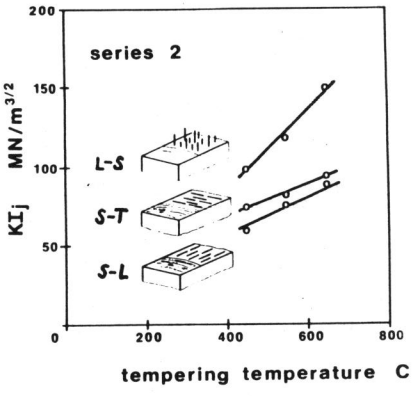

Fig.8: Influence of inclusion orientation on the crack toughness

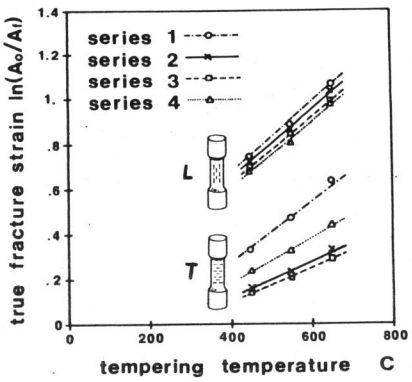

Fig.9:Ductility of specimens with different inclusion distributions

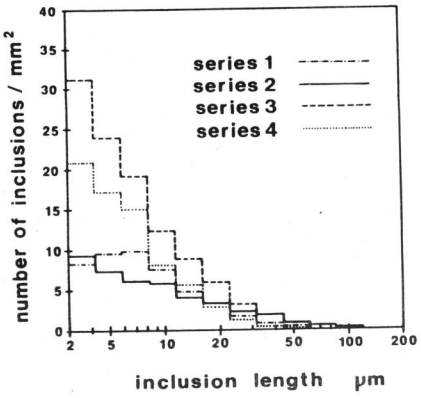

Fig.10: Incusion distributions in the four series